Open Research Online

The Open University's repository of research publications and other research outputs

Observations of the *Hubble Deep Field* with the *Infrared Space Observatory* - V. Spectral energy distributions, starburst models and star formation history

Journal Item

How to cite:

Rowan-Robinson, M.; Mann, R. G.; Oliver, S. J.; Efstathiou, A.; Eaton, N.; Goldschmidt, P.; Mobasher, B.; Serjeant, S. B. G.; Sumner, T. J.; Danese, L.; Elbaz, D.; Franceschini, A.; Egami, E.; Kontizas, M.; Lawrence, A.; McMahon, R.; Norgaard-Nielsen, H. U.; Perez-Fournon, I. and Gonzalez-Serrano, J. I. (1997). Observations of the Hubble Deep Field with the Infrared Space Observatory - V. Spectral energy distributions, starburst models and star formation history. Monthly Notices of the Royal Astronomical Society, 289(2) pp. 490–496.

For guidance on citations see FAQs.

© 1997 Royal Astronomical Society

https://creativecommons.org/licenses/by-nc-nd/4.0/

Version: Version of Record

Link(s) to article on publisher's website:
http://dx.doi.org/doi:10.1093/mnras/289.2.490
http://dx.doi.org/10.1093/mnras/289.2.490

Copyright and Moral Rights for the articles on this site are retained by the individual authors and/or other copyright owners. For more information on Open Research Online's data policy on reuse of materials please consult the policies page.

oro.open.ac.uk

1997MNRAS.289..490R

Mon. Not. R. Astron. Soc. **289**, 490–496 (1997)

Observations of the *Hubble Deep Field* with the *Infrared Space Observatory* – V. Spectral energy distributions, starburst models and star formation history

M. Rowan-Robinson,[1] R. G. Mann,[1] S. J. Oliver,[1] A. Efstathiou,[1] N. Eaton,[1] P. Goldschmidt,[1] B. Mobasher,[1] S. B. G. Serjeant,[1] T. J. Sumner,[1] L. Danese,[2] D. Elbaz,[3] A. Franceschini,[4] E. Egami,[5] M. Kontizas,[6] A. Lawrence,[7] R. McMahon,[8] H. U. Norgaard-Nielsen,[9] I. Perez-Fournon[10] and J. I. Gonzalez-Serrano[11]

[1] *Astrophysics Group, Imperial College London, Blackett Laboratory, Prince Consort Road, London SW7 2BZ*
[2] *SISSA, Via Beirut 2-4, Trieste, Italy*
[3] *Service d'Astrophysique, Saclay, 91191, Gif-sur-Yvette Cedex, France*
[4] *Osservatorio Astronomico di Padova, Vicolo dell'Osservatorio 5, I-35 122, Padova, Italy*
[5] *Max-Planck-Institut für Extraterrestrische Physik, Giessenbachstrasse, D-8046, Garching bei Munchen, Germany*
[6] *Astronomical Institute, National Observatory of Athens, PO Box 200048, GR-118 10, Athens, Greece*
[7] *Institute for Astronomy, University of Edinburgh, Blackford Hill, Edinburgh EH9 3HJ*
[8] *Institute of Astronomy, The Observatories, Madingley Road, Cambridge CB3 0HA*
[9] *Danish Space Research Institute, Gl. Lundtoftevej 7, DK-2800 Lyngby, Copenhagen, Denmark*
[10] *Instituto de Astrofisica de Canarias, Via Lactea, E-38200 La Laguna, Tenerife, Canary Islands, Spain*
[11] *Instituto de Fisica de Cantabria, Santander, Spain*

Accepted 1997 May 9. Received 1997 March 24; in original form 1996 December 5

ABSTRACT

We have modelled the spectral energy distributions of the 13 *Hubble Deep Field* (HDF) galaxies reliably detected by the *Infrared Space Observatory* (*ISO*). For two galaxies the emission detected by *ISO* is consistent with being starlight or the infrared 'cirrus' in the galaxies. For the remaining 11 galaxies there is a clear mid-infrared excess, which we interpret as emission from dust associated with a strong starburst. 10 of these galaxies are spirals or interacting pairs, while the remaining one is an elliptical with a prominent nucleus and broad emission lines.

We give a new discussion of how the star formation rate can be deduced from the far-infrared luminosity, and derive star formation rates for these galaxies of 8–1000ϕ $M_{\odot}$ yr^{-1}, where ϕ takes account of the uncertainty in the initial mass function. The HDF galaxies detected by *ISO* are clearly forming stars at a prodigious rate compared with nearby normal galaxies. We discuss the implications of our detections for the history of star and heavy element formation in the Universe. Although uncertainties in the calibration, reliability of source detection, associations and starburst models remain, it is clear that dust plays an important role in star formation out to redshift 1 at least.

Key words: stars: formation – galaxies: evolution – galaxies: starburst – cosmology: observations – infrared: galaxies.

1 INTRODUCTION

Because of its great depth and high resolution, and the intensive follow-up which has been carried out on it, the *Hubble Deep Field* (HDF) is an exceptional resource for cosmological studies. The central area of the HDF consists of 5×5 arcmin^2 of sky. It was imaged by the *Hubble Space Telescope* on 150 orbits in 1995 December and reaches to at least 29th magnitude in *I* (800 nm), *V* (600 nm) and *B* (450 nm), and to 27th magnitude in *U* (300 nm) (Williams et al. 1996). We were successful in bidding for Director's Time on the *Infrared Space Observatory* (*ISO*), and were awarded a

© 1997 RAS

Downloaded from http://mnras.oxfordjournals.org/ at Open University Library (PER) on April 13, 2016

© Royal Astronomical Society • Provided by the NASA Astrophysics Data System

1997MNRAS.289..490R

total of 12.5 h to map the HDF with ISOCAM in the LW2 (6.7 μm) and LW3 (15 μm) filters. The observations were carried out in 1996 July and have been described by Serjeant et al. (1997, hereafter Paper I). The images have been searched for point sources by Goldschmidt et al. (1997, hereafter Paper II): a total of 15 sources were found in the central HDF area at 6.7 μm, and five at 15 μm, of which six and four, respectively, are from complete and reliable sub-samples. A further 27 sources were found in the *Flanking Fields* around the HDF. The resulting source counts have been discussed by Oliver et al. (1997, hereafter Paper III) and shown to be consistent with the strongly evolving starburst models previously used to model the 60-μm and 1.4-GHz counts (Rowan-Robinson et al. 1993; Franceschini et al. 1994; Pearson & Rowan-Robinson 1996). Associations for the 17 *ISO* sources in the central HDF area (two were detected at both 6.7 and 15 μm) were sought with HDF galaxies using a likelihood method (Mann et al. 1997, hereafter Paper IV) and 13 credible associations were found. In this paper we take the view that these associations tentatively confirm the reality of those sources that are not in the reliable and complete sub-samples. There is ambiguity about some of the associations (Paper IV), and in some cases the *ISO* flux may be due to more than one galaxy (this is particularly so for the 15-μm detections). In this paper we have assumed that all the flux is assigned to the galaxy with the highest likelihood. This assumption does not have a great effect on our overall conclusions. For the two sources for which the likelihoods did not completely resolve ambiguities (123643.0 + 621152 and 123648.4 + 621215), we have conservatively chosen the lower redshift galaxy as the association.

In this paper we discuss the spectral energy distribution (SED) of the 13 galaxies detected by *ISO* in the central HDF area, and consider the implications for star formation rates and the overall history of star formation in the Universe. Details of the 13 galaxies are given in Table 1.

A striking feature of the fainter HDF galaxies is their blue colours, indicative of high-redshift galaxies undergoing bursts of star formation. This is confirmed both by systematic analyses of the colours of the HDF galaxies (Mobasher et al. 1996) and by studies of the morphologies of the galaxies (Abraham et al. 1996), which show a high proportion of interacting and merging systems. In both respects the HDF galaxies look like a higher redshift version of the starburst galaxies found by *IRAS*. This was one of the strong motivations for seeking observing time with *ISO*. The fact that HDF galaxies have been detected by *ISO* is sufficient to demonstrate that this analogy with *IRAS* galaxies is highly relevant.

An Einstein–de Sitter model ($\Omega_0 = 1$), with a Hubble constant $H_0 = 50$ km s^{-1} Mpc^{-1}, has been used throughout the paper.

2 SPECTRAL ENERGY DISTRIBUTIONS

For the 13 galaxies reliably detected by *ISO* in the HDF (Paper II; Paper IV), we have modelled the SEDs from 0.3 to 15 μm. Spectroscopic redshifts are available for nine of the galaxies (Cowie 1996; Cohen et al. 1996; Phillips et al. 1997). For the remaining four we have used photometric redshifts determined by the method of Mobasher et al. (1996). The latter analysis has been repeated using the total magnitudes and colours given in the STScI HDF catalogue (Williams et al. 1996). The resulting redshifts agree well with those determined in a small, fixed aperture by Mobasher et al. (1996).

The *U, B, V, I* data (*AB* magnitudes) from *HST* and the *J, H*/*K* data of Cowie (1996) have been fitted with galaxy models from the library of Bruzual & Charlot (1993). The near-infrared data were corrected to the same aperture as the optical data. For wavelengths beyond 2.5 μm, the Bruzual & Charlot models give predictions based on *IRAS* data for their standard stars, which appear to generate a spurious secondary peak at 12 μm (even for the youngest starburst models). We have therefore replaced the Bruzual & Charlot predictions with a Rayleigh–Jeans extrapolation beyond 2.5 μm. Excellent fits to the *U* to *K* data for our galaxies can be obtained using models with starbursts of duration 10^9 yr, viewed at a range of subsequent times $\tau = 1$ to 2.4 Gyr

Table 1. 60-μm luminosities and star formation rates for *ISO* HDF galaxies.

	Galaxy (ISOHDF)	redshift	τ (Gyr)	$L_{0.3}/L_\odot$	$L_{0.8}/L_\odot$	$L_{15}/L_\odot$	$L_{60}/L_\odot$	$(\dot{M}_{*,all}/M_\odot)$ xϕ^{-1}	notes
1	12 36 41.1 +62 11 29	(0.047)	1.02	2.8×10^8	4.0×10^8	2.1×10^8	7.6×10^8	0.20	S sb c
2	12 36 41.6 +62 11 42	0.585	1.14	2.8×10^9	7.3×10^9	1.1×10^{11}	3.9×10^{11}	101	I sb b,d
3	12 36 42.6 +62 12 10	0.454	1.14	6.9×10^9	1.8×10^{10}	1.7×10^{10}	6.0×10^{10}	16	S sb b
4	12 36 42.9 +62 13 09	(0.74)	1.14	5.5×10^9	1.4×10^{10}	5.3×10^{11}	1.9×10^{12}	495	S sb b
5	12 36 43.0 +62 11 52	(0.82)	2.4	3.4×10^9	3.0×10^{10}	8.9×10^{11}	3.2×10^{12}	840	S sb a
6	12 36 43.7 +62 12 55	0.558	1.14	1.4×10^{10}	3.6×10^{10}	8.6×10^{10}	3.1×10^{11}	80	I sb c,e
7	12 36 43.9 +62 11 30	1.01	3.5	1.75×10^{10}	1.35×10^{11}	2.0×10^{10}	1.4×10^{11}	-	E sl b,e
8	12 36 46.4 +62 14 06	0.960	1.28	2.2×10^{10}	8.1×10^{10}	1.1×10^{12}	3.9×10^{12}	1010	E sb a,e
9	12 36 48.1 +62 14 32	(0.023)	1.14	6.0×10^7	1.5×10^8	1.8×10^7	1.26×10^8	-	E cirr a,c
10	12 36 48.4 +62 12 15	(0.778)	1.02	4.5×10^9	1.15×10^{10}	6.8×10^{11}	2.45×10^{12}	640	S sb a
11	12 36 49.7 +62 13 15	0.475	1.28	1.75×10^9	1.26×10^{10}	9.5×10^{10}	3.4×10^{11}	88	S sb a,c,e
12	12 36 51.5 +62 13 57	0.557	1.14	4.7×10^9	2.7×10^{10}	5.2×10^{10}	1.86×10^{11}	48	S sb d
13	12 36 58.9 +62 12 48	0.320	1.02	2.4×10^9	6.0×10^9	9.0×10^9	3.2×10^{10}	8	S sb a

S – spiral; E – elliptical; I – interacting pair; sb – SED fitted with starburst model; cirr – SED fitted with cirrus model; sl – SED fitted with starlight; a – detected at 6.7 μm, from reliable and complete sub-sample; b – detected at 6.7 μm, from supplementary list; c – detected at 15 μm, from reliable and complete sub-sample; d – detected at 15 μm, from supplementary list; e – detected at 1.4 GHz (Fomalont et al. 1997).

Downloaded from http://mnras.oxfordjournals.org/ at Open University Library (PER) on April 13, 2016

© Royal Astronomical Society • Provided by the NASA Astrophysics Data System

1997MNRAS.289..490R

(values of τ are given in Table 1). In the case of the galaxies for which we have only photometric redshifts, the good fits of the models to the data provide support for the photometric redshifts. Almost equally good fits could be obtained with an exponentially decreasing star formation rate with a time-scale of 1 Gyr. No allowance is made for reddening at this stage. For one galaxy (123643.9 + 621130), the 6.7-μm emission can be accounted for almost completely by starlight.

For the remaining 12 galaxies, there is a clear excess of infrared radiation. We have considered first the possibility that we are seeing the infrared 'cirrus' in the galaxies, emission from starlight in the galaxies absorbed by interstellar grains and re-emitted in the infrared. The cirrus models of Rowan-Robinson (1992) have been revised to incorporate very small grains and polycyclic aromatic hydrocarbons (PAHs) correctly (Efstathiou & Rowan-Robinson, in preparation). For 11 of the galaxies, there was no plausible cirrus model, because the resulting far-infrared luminosity was always at least three times the total optical–UV luminosity of the galaxy. A typical value of $L_{\rm FIR}/L_{\rm opt\text{-}UV}$ for cirrus emission is 0.2–0.3 (Rowan-Robinson et al. 1987; Rowan-Robinson 1992). For one galaxy (123648.1 + 621432), in which the cirrus model gave a far-infrared luminosity comparable to that seen in the optical and UV, we accepted the cirrus model fit (see Fig. 1).

Fig. 1 shows fits of the standard starburst model of Efstathiou & Rowan-Robinson (in preparation) to the infrared SEDs of the remaining 11 *ISO*-detected HDF galaxies. The model is a development of the earlier starburst model of Rowan-Robinson & Efstathiou (1993), with a proper treatment of very small grains and PAHs, and gives an excellent fit to the spectra of M82 and the starburst galaxy NGC 6090 studied by *ISO* (Acosta-Pulido et al. 1996). Although in most cases we have only a single mid-infrared data point, it is satisfactory that, in the case where we have detections at both 6.7 and 15 μm, the model fits both data points well. where only upper limits are available at one of the *ISO* wavelengths, these are generally consistent with the predictions of the model [for objects 4 and 5 in Table 1, the upper limits at 15 μm may imply that the model parameters need adjustment, that an alternative model, e.g. a dusty active galactic nucleus (AGN) torus, may be needed, or that the 6.7-μm detection is unreliable]. Even more impressive is the fit for three galaxies to the VLA detections by Fomalont et al. (1997), for which we have assumed in the model the standard radio–far-infrared correlation [S(60 μm)/S(1.4 GHz) = 90] and a radio spectral index of 0.8. This

Downloaded from http://mnras.oxfordjournals.org/ at Open University Library (PER) on April 13, 2016

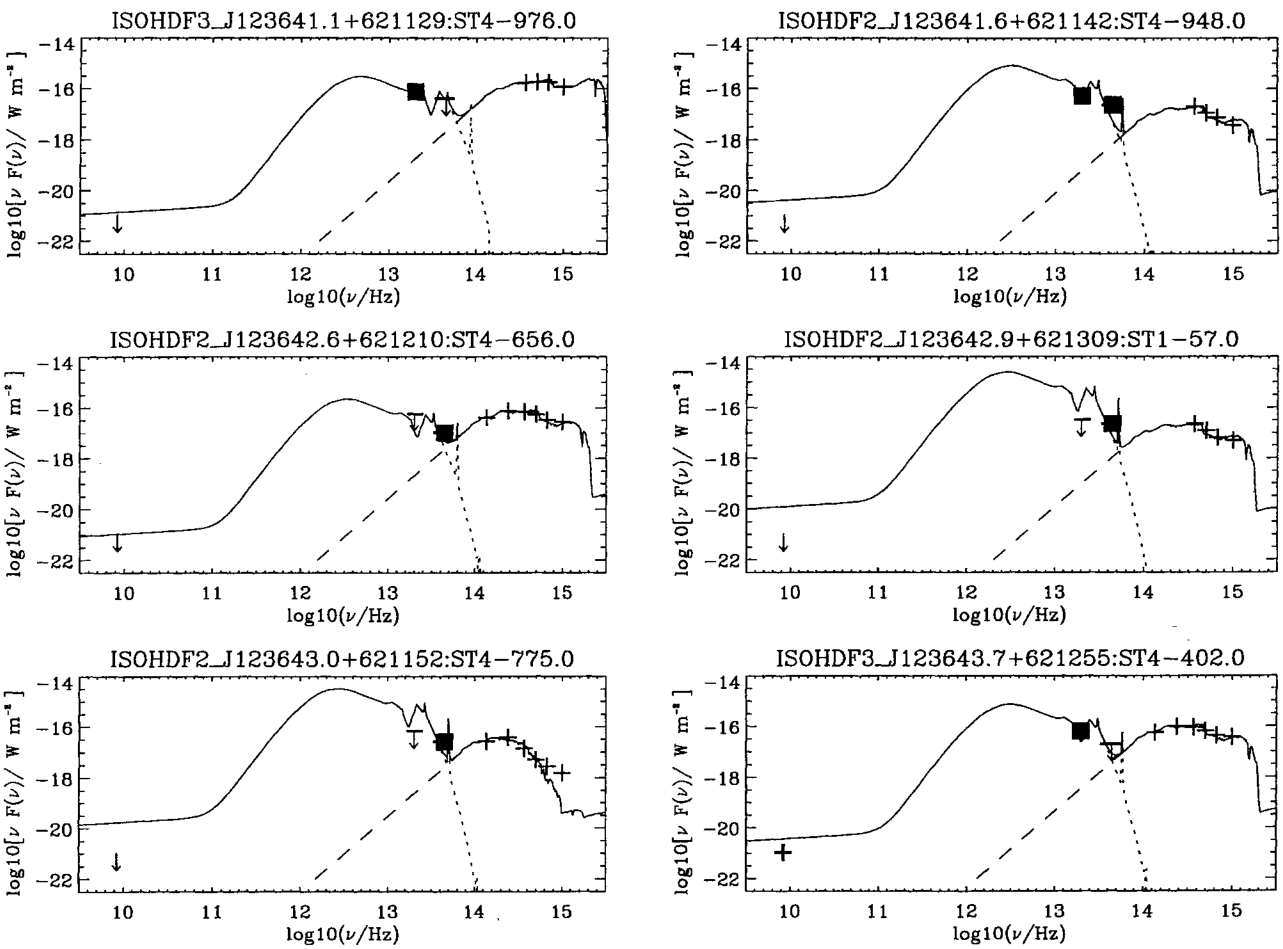

Figure 1. Spectral energy distributions [$\nu F(\nu)$ in W m^{-2}] for the galaxies of Table 1, in order of right ascension, compared with the Bruzual & Charlot (1993) models (optical and near infrared) and the Efstathiou et al. (in preparation) cirrus and starburst models (mid- and far-infrared). Crosses: *HST*, IFA and VLA data; filled squares: *ISO* data.

© Royal Astronomical Society • Provided by the NASA Astrophysics Data System

1997MNRAS.289..490R

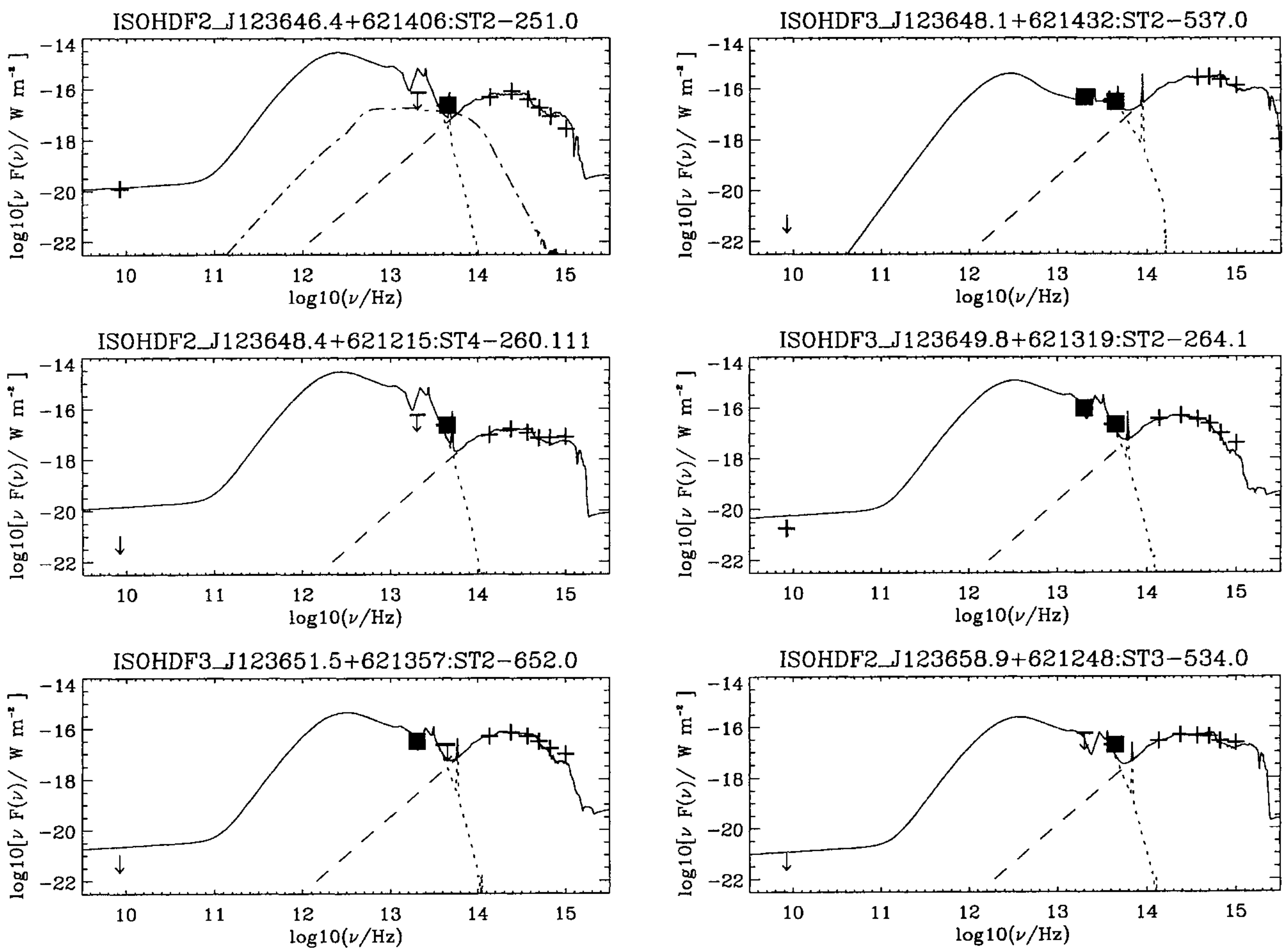

Figure 1 – *continued*

supports the idea that we really are seeing dust emission starbursts with *ISO*. In most other cases the models are consistent with the 1.4-GHz upper limit, taken as 12.2 μJy (Fomalont et al. 1997) (but for objects 4, 5 and 10, the radio limits lie significantly below the predictions of the starburst model). If we look at the morphologies of the galaxies in our sample, the two non-starburst galaxies are both ellipticals. Of the 11 galaxies whose SEDs we fit as starbursts, eight are spirals, two are interacting pairs and one is a galaxy (possibly spiral) with a prominent nucleus (123646.4 + 621406). Broad lines have been found in the optical spectrum of this galaxy, and it is possible that the 6.7-μm emission could be from a dusty torus surrounding the AGN, rather than from a starburst. However, if this interpretation were correct, the agreement of the radio flux with the prediction of the starburst model would be a coincidence. There are several other objects in which a dusty torus model would give an equally satisfactory fit to the observed infrared excess. However, since the covering factor by dust in AGN is generally found to be <0.5 (Rowan-Robinson 1995), it is unlikely that more than one object in our sample is an AGN with its dust torus seen edge-on. The source count models discussed by Oliver et al. (Paper III) predict that the fraction of AGN expected in 6.7- and 15-μm samples should be small. We therefore assume that the infrared excess in the remaining 11 objects is from starbursts rather than from AGN with dusty tori.

Table 1 gives the inferred rest-frame values of νL_ν at 0.3, 0.8, 15 and 60 μm. It can be seen that $L_{60}/L_{0.8}$ ranges from 2 to 200, and $L_{60}/L_{0.3}$ ranges from 3 to 1000. Thus the implication of the *ISO* detections is that, at least for the detected galaxies, the bulk of the bolometric luminosity of the galaxies is emitted at far-infrared wavelengths. The interpretation of this is similar to that for the starburst galaxies found in the *IRAS* surveys: most massive star formation takes place in dense molecular clouds and is shrouded from view by a substantial optical depth in dust. What is seen in the optical and UV represents stars formed near the edges of the clouds, so that the light from these stars can escape directly.

3 STAR FORMATION RATE

A number of authors have discussed how the star formation rate in a galaxy can be inferred from its optical, ultraviolet or far-infrared luminosity. Scoville & Young (1983) estimated the star formation rate of O, B and A stars ($M > 1.6\,\mathrm{M}_\odot$) from the total far-infrared luminosity of galaxies, implicitly assuming that a burst of star formation lasts 10^9 yr, finding

$$\dot{M}_{*,\mathrm{OBA}} = 7.7\times10^{-11} L_{\mathrm{FIR}}/\mathrm{L}_\odot. \qquad (1)$$

Thronson & Telesco (1986) used a Salpeter initial mass

© Royal Astronomical Society • Provided by the NASA Astrophysics Data System

Downloaded from http://mnras.oxfordjournals.org/ at Open University Library (PER) on April 13, 2016

1997MNRAS.289..490R

function (IMF) to give rates of star formation of all stars and of OBA stars, averaged over the past 2×10^6 yr, per unit far-infrared luminosity:

$$\dot{M}_{*,\mathrm{OBA}} = 2.1 \times 10^{-10} L_{\mathrm{FIR}}/\mathrm{L}_{\odot}, \tag{2}$$

$$\dot{M}_{*,\mathrm{all}} = 6.5 \times 10^{-10} L_{\mathrm{FIR}}/\mathrm{L}_{\odot}. \tag{3}$$

They attributed the fact that (2) is a factor of 3 higher than (1) to the different assumptions about the duration of the burst. They also gave the scaling factors for the star formation rate between the different IMFs and lower mass limits:

M/L (Miller–Scalo, 100, 0.1): M/L (Miller–Scalo, 100, 1.6):

M/L (Salpeter, 100, 0.1): M/L (Salpeter, 100, 1.6)

$= 10.2:4.0:3.1:1.$

More recently, Madau et al. (1996) have calculated total star formation rates and heavy element production, $\dot{M}_Z$, from the ultraviolet luminosity densities at 2800 Å, using a Salpeter IMF and the evolutionary models of Bruzual & Charlot (1993). The figures they give are equivalent to

$$\dot{M}_{*,\mathrm{all}} = 5.3 \times 10^{-10} L_{2800}/\mathrm{L}_{\odot}, \tag{4}$$

$$\dot{M}_{*,\mathrm{all}} = 42 \dot{M}_Z. \tag{5}$$

To convert from 60-μm luminosity to star formation rate, we assume that a fraction ε ($\simeq 1$) of the optical and UV energy emitted in a starburst is absorbed by dust and emitted in the far-infrared, so that

$$L_{\mathrm{bol,FIR}} = \varepsilon L_{\mathrm{bol,opt\text{-}UV}}. \tag{6}$$

The bolometric correction at 2800 Å for the 1-Gyr starburst models of Bruzual & Charlot (1993), when viewed at early ages, is 3.5, and those at 15 and 60 μm for the dusty starburst model of Rowan-Robinson & Efstathiou (1993) are 6.0 and 1.7, respectively, so, using (4) and (6):

$$\begin{aligned} \dot{M}_{*,\mathrm{all}}/[L_{60}/\mathrm{L}_{\odot}] &= 2.6\phi/\varepsilon \times 10^{-10}, \\ \dot{M}_{*,\mathrm{all}}/[L_{15}/\mathrm{L}_{\odot}] &= 9.3\phi/\varepsilon \times 10^{-10}, \end{aligned} \tag{7}$$

where the factor of ϕ incorporates (1) the correction from a Salpeter IMF to the true IMF ($\times 3.3$ if the Miller–Scalo IMF is the correct one), (2) a correction if the starburst event is forming only massive stars ($\times 1/3.1$ if only O, B, A stars, > 1.6 $\mathrm{M}_{\odot}$, are being formed). This estimate, which is now based on detailed starburst models for the optical–UV radiation and proper radiative transfer models for the far-infrared emission, is a factor of 1.9 higher than that of Scoville & Young (1983, equation 1 above) and 0.7 times that of Thronson & Telesco (1986, equations 2 and 3 above).

4 STAR FORMATION RATES FOR *ISO* HDF GALAXIES

Table 1 gives the inferred 15- and 60-μm luminosities, and star formation rates based on equation (7), for the 11 HDF starburst galaxies detected by *ISO*. the star formation rates range (with one exception) from 8 to 1000 ϕ $\mathrm{M}_{\odot}$ yr^{-1}. The galaxies detected by *ISO* are forming stars at a prodigious rate compared with nearby normal spirals. Although star formation rates based only on 6.7- and 15-μm detections are bound to be rather uncertain, because most of the energy is emitted at much longer wavelengths, it is clear that the star formation rates deduced from the UV fluxes detected by *HST* are a severe underestimate for these galaxies.

It is of course of interest to ask whether these star formation rates can be typical of all the galaxies in the HDF. For two of the galaxies detected by *ISO*, the 6.7- and/or 15-μm flux is consistent with emission from starlight and/or cirrus, and there is no evidence for a luminous starburst. For other bright galaxies in the HDF, the non-detection by *ISO* gives a significant upper limit on any excess far-infrared emission. For these galaxies the estimates of star formation rate from the UV flux will be correct. However, we cannot rule out the possibility that, for a significant fraction of the fainter HDF galaxies, particularly those with $z > 1$, the presence of a strong far-infrared excess is the norm rather than the exception. When we see star formation within our Galaxy or in other nearby galaxies, the bulk of the massive stars (which produce all the heavy elements and most of the ultraviolet light) are formed within dense molecular clouds behind a high optical depth in dust. The starburst galaxies detected by *IRAS* emit most of their radiation at far-infrared wavelengths. It is a reasonable expectation that as we look back to epochs when the bulk of the stars in a galaxy are formed, this too will take place within dense clouds of molecules and dust and be primarily a far-infrared phenomenon. Of course, eventually we will see back to epochs when the very first stars form, when little or no heavy elements or dust are present, and star formation will be entirely an optical and UV phenomenon. However, this transparent phase may last no more than a few per cent of the main star formation phase, say 10^7–10^8 yr, and be confined to very high redshifts (> 3–5).

5 INFRARED LUMINOSITY DENSITY AND THE HISTORY OF STAR FORMATION

Madau et al. (1996) have used the Canada-France Redshift Survey (Lilly et al. 1996) and HDF data to calculate the history of star formation and heavy element generation, under the assumption that the UV gives a complete view of the star formation that is occurring. Integrating over the star formation density as a function of redshift, they conclude that all the heavy elements associated with the visible matter in galaxies can be generated. However, if their calculated baryonic density is converted to a value for Ω_0, a value of 0.0035 is obtained, only 7 per cent of the baryonic density of 0.05, for an assumed $H_0 = 50$ km s^{-1} Mpc^{-1}, derived from cosmological nucleosynthesis of the light elements (Walker et al. 1991). It is not unreasonable to assume that some of the remaining 93 per cent of baryons has participated in star formation and heavy element production. For example, the hot gas in clusters is known to have a heavy element abundance of at least one-third of solar.

We first estimate the far-infrared luminosity density for the luminosity function derived from *IRAS* 60-μm data. Oliver et al. (Paper III) have shown that the 6.7- and 15-μm source counts are consistent with the strongly (luminosity)-evolving starburst models which we have used to fit (1) the redshift distribution in *IRAS* redshift surveys (Saunders et al. 1990; Oliver et al. 1995), (2) the 60-μm source counts

Downloaded from http://mnras.oxfordjournals.org/ at Open University Library (PER) on April 13, 2016

© Royal Astronomical Society • Provided by the NASA Astrophysics Data System

1997MNRAS.289..490R

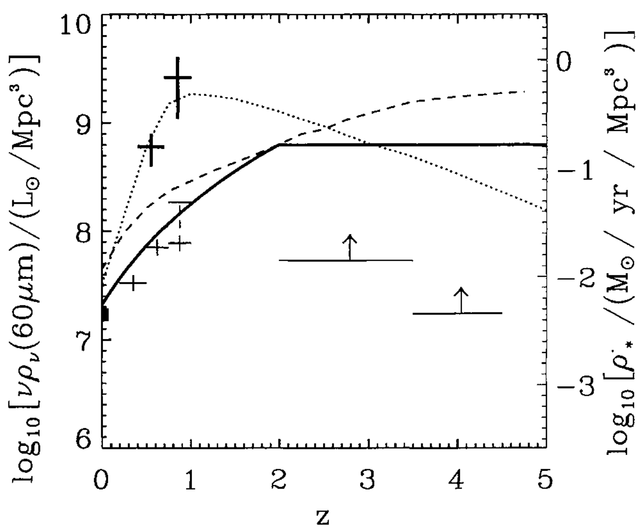

Figure 2. The luminosity density at 60 μm as a function of redshift (left-hand scale) and the star formation rate (right-hand scale, from equation 7 assuming $\phi=1$). The solid curve is derived from the *IRAS* 60-μm luminosity function of Saunders et al. (1990), assuming evolution of the form (8). The broken curve is the model of Franceschini et al. (1994 and in preparation) and the dotted curve is the infall model of Pei & Fall (1995) with $\Omega_g = 0.008^{-1}$. The thick crosses are the estimates of the luminosity density derived directly from the *ISO* data for the galaxies of Table 1. Also shown (thin crosses and lower limits) are the star formation rates derived from the ultraviolet (2800 Å) luminosity density by Madau et al. (1996).

(Pearson & Rowan-Robinson 1996), (3) the far-infrared background, including the claimed detection using FIRAS data from *COBE* by Puget et al. (1996) (Pearson & Rowan-Robinson 1996; Rowan-Robinson & Pearson 1996), and (4) the sub-mJy 1.4-GHz radio counts (Rowan-Robinson et al. 1993; Hopkins et al. 1996).

The solid curve in Fig. 2 shows the luminosity density at 60 μm as a function of redshift. For $z<0.3$ this is directly derived from *IRAS* galaxy redshift surveys [the luminosity function given in line (23) of table 3 of Saunders et al. (1990)]. The extrapolation to higher redshift is the luminosity evolution model used in Pearson & Rowan-Robinson (1996), Rowan-Robinson et al. (1993) and Oliver et al. (Paper III) to fit the deep 60-μm and 1.4-GHz source counts, for which

$$L_*(z)=(1+z)^{3.1}, \qquad z>2,$$
$$L_*(z)=3^{3.1}, \qquad 2\le z<5. \tag{8}$$

Using equation (7), we can convert this to a density of star formation, and integrate to derive a total mass density in stars or in heavy elements. We find

$$\Omega_* = 0.008 h_{50}^{-2}\phi, \qquad \Omega_Z = 0.000\,19 h_{50}^{-2}. \tag{9}$$

These values are not unreasonable. They require that twice as much star formation as has been inferred by Madau et al. (1996) from the UV integrated light has taken place shrouded by dust. The total fraction of baryonic matter that has participated in star formation would be of the order of 20 per cent, with about one-third of the resulting heavy elements now residing in the luminous parts of galaxies. The remainder could be in baryonic objects in the haloes of galaxies or in intergalactic gas (including the hot X-ray-emitting gas in clusters). In fact, evolutionary rates appreciably steeper than that assumed in equation (8) can probably not be ruled out at this stage. If the star-forming galaxies that we have detected with *ISO* are typical of the fainter HDF galaxies, then we may require that more than 50 per cent of baryons have participated in star formation and heavy element production, presumably with a truncated IMF so that most of the baryons now reside in dark remnants. Similar conclusions are reached if we use the model for evolution of infrared galaxies of Franceschini et al. (1994 and in preparation), shown as a broken line in Fig. 2.

We have also estimated the contribution to the 60-μm luminosity density implied directly by the *ISO* HDF starburst galaxies. There are five starburst galaxies in the redshift bin 0.4–0.7 and three in the redshift bin 0.7–1.0 (we have omitted the galaxy with broad lines). Estimating the volume of the Universe sampled by the HDF survey, we find contributions of $(6.0\pm2.0)\times10^8$ and $(2.6\pm1.5)\times10^9$ $L_\odot$ Mpc^{-3} for the redshift ranges 0.4–0.7 and 0.7–1.0 respectively. These estimates take no account of sources fainter than the *ISO* limit, and they are subject to any uncertainty in the *ISO* calibration (probably a factor of 50 either way), as well as the considerable uncertainty associated with extrapolating from 6.7 and 15 μm to 60 μm, so must be seen as very preliminary. They appear to be significantly higher than the predictions for evolution of the form (8) (the solid line in Fig. 3) by factors of 5 and 10 respectively. This may imply that the evolution of starburst galaxies is steeper than assumed in equation (8) for $0<z<1$. Alternatively, our models may overestimate the 60-μm luminosities for at least some of the galaxies, for example because the 6.7- and 15-μm radiation comes from dust tori around AGN.

We have also shown in Fig. 2 one of the more extreme of the models of Pei & Fall (1995, dotted line). This illustrates that the luminosity density estimated from the *ISO* HDF galaxies is not at odds with current data on the number density of quasar absorption-line clouds or the observed heavy element abundance at high redshift. However, for this model $\Omega_* = 0.032 h_{50}^{-1}\phi$, $\Omega_Z = 0.000\,76 h_{50}^{-1}$, which would probably imply that only higher mass stars were being formed in the *ISO* HDF galaxies.

Support for the idea that stronger evolution than equation (8) is required for the starburst galaxy population comes from the fit to the *ISO* counts by Oliver et al. (Paper III). The Pearson & Rowan-Robinson (1996) model fails to predict a strong enough contribution to the counts by starburst galaxies. The Franceschini et al. (1994) model, involving a strongly evolving starburst population in elliptical galaxies, appears to give a better fit to the *ISO* counts. This idea can be tested by the deep 90-μm surveys which we and others are carrying out with *ISO*. It will also be interesting to observe the HDF galaxies detected by *ISO* at submillimetre wavelengths, for example with SCUBA at the JCMT.

6 CONCLUSIONS

We have modelled the spectral energy distributions of the 13 galaxies reliably associated with *ISO* sources detected at 6.7 and/or 15 μm. For two galaxies the emission detected by *ISO* is consistent with being starlight or normal infrared

Downloaded from http://mnras.oxfordjournals.org/ at Open University Library (PER) on April 13, 2016

© Royal Astronomical Society • Provided by the NASA Astrophysics Data System

1997MNRAS.289..490R

'cirrus' in the galaxies. For the remaining 11 galaxies there is a strong mid-infrared excess, which we interpret as emission from dust associated with a strong starburst. In three cases the starburst model appears to be confirmed by the good agreement of the predicted radio flux with that detected by Fomalont et al. (1997). Inferred rest-frame luminosities (νK_ν) at 0.3, 0.8, 15 and 60 μm are given, and $L_{60}/L_{0.3}$ ranges from 3 to 1000 for the 11 galaxies. Thus most of the bolometric luminosity of the galaxies is predicted to emerge at far-infrared wavelengths.

We give a new discussion of how the star formation rate can be deduced from the far-infrared luminosity, and derive star formation rates of 8–1000 ϕ $M_\odot$ yr^{-1}, where ϕ takes account of the uncertainty in the initial mass function (=1 for a Salpeter IMF). The HDF galaxies detected by *ISO* are clearly forming stars at a prodigious rate compared with nearby normal galaxies. We discuss the implications of our detections, and of the *IRAS* 60-μm luminosity function and evolution, for the history of star and heavy element formation in the Universe. We conclude that at least 20 per cent of baryons must have participated in star formation.

Further information on the *ISO* HDF project can be found on the *ISO* HDF World Wide Web page (http://artemis.ph.ic.au.uk/hdf/).

ACKNOWLEDGMENTS

This paper is based on observations with *ISO*, an ESA project with instruments funded by ESA member states (especially the PI countries: France, Germany, the Netherlands and the United Kingdom) and with the participation of ISAS and NASA. We thank the referee, Harry Ferguson, for comments and suggestions which enabled us to improve this paper. This work was supported by PPARC (Grant No. GR/K98728) and by the EC TMR Network Programme (contract No. FMRX-CT96-0068).

REFERENCES

Abraham R. G., Tanvir N. R., Santiago B. X., Ellis R. S., Glazebrook K., van den Bergh S., 1996, MNRAS, 279, L47
Acosta-Pulido J. A. et al., 1996, A&A, 315, L121
Bruzual A. G., Charlot S., 1993, ApJ, 405, 538
Cohen J. G., Cowie L. L., Hogg D. W., Songaila A., Blandford R., Hu E. M., Shopbell P., 1996, ApJ, 471, L5
Cowie L. L., 1996, http:/www.ifa.hawaii.edu/cowie/hdf.html
Fomalont E. B., Kellermann K. I., Richards E. B., Windhorst R., Partridge R. B., 1997, ApJ, 475, L5
Franceschini A., Mazzei P., De Zotti G., Danese L., 1994, ApJ, 427, 140
Goldschmidt P. et al., 1997, MNRAS, 289, 465 (Paper II, this issue)
Hopkins A., Mobasher B., Cram L., Rowan-Robinson M., 1997, MNRAS, in press
Lilly S. J., Le Fevre O., Hammer F., Crampton D., 1996, ApJ, 460, L1
Madau P., Ferguson H. C., Dickinson M. E., Giavalisco M., Steidel C. C., Fruchter A., 1996, MNRAS, 283, 1388
Mann R. G. et al., 1997, MNRAS, 289, 482 (Paper IV, this issue)
Mobasher B., Rowan-Robinson M., Georgakakis A., Eaton N., 1996, MNRAS, 282, L7
Oliver S. et al., 1995, in Maddox S. J., Aragon-Salamanca A., eds, Proc. 35th Herstmonceux Conf., Wide-Field Spectroscopy and the Distant Universe. World Scientific, Singapore, p. 274
Oliver S. J. et al., 1997, MNRAS, 289, 471 (Paper III, this issue)
Pearson C., Rowan-Robinson M., 1996, MNRAS, 283, 174
Pei Y. C., Fall S. M., 1995, ApJ, 454, 69
Phillips A. C., Guzman R., Gallego J., Koo D. C., Lowenthal J. D., Vogt N. P., Faber S. M., Illingworth G. D., 1997, ApJ, in press
Puget J.-L., Abergal A., Bernard J.-P., Boulanger F., Burton W. B., Désert F.-X., Hartmann D., 1996, A&A, 308, 5
Rowan-Robinson M., 1992, MNRAS, 258, 787
Rowan-Robinson M., 1995, MNRAS, 272, 737
Rowan-Robinson M., Efstathiou A., 1993, MNRAS, 263, 675
Rowan-Robinson M., Pearson C., 1996, in Dwek E., ed., Unveiling the Infrared Background. Am. Inst. Phys., New York, p. 192
Rowan-Robinson M., Helou G., Walker D., 1987, MNRAS, 227, 589
Rowan-Robinson M., Benn C. R., Lawrence A., McMahon R. G., Broadhurst T. J., 1993, MNRAS, 263, 123
Saunders W., Rowan-Robinson M., Lawrence A., Efstathiou G., Kaiser N., Ellis R. S., Frenk C. S., 1990, MNRAS, 242, 318
Scoville N. Z., Young J. S., 1983, ApJ, 265, 148
Serjeant S. et al., 1997, MNRAS, 289, 457 (Paper I, this issue)
Thronson H., Telesco C., 1986, ApJ, 311, 98
Walker T. P., Steigman G., Schramm D. N., Olive K. A., Kang H.-S., 1991, ApJ, 376, 51
Williams R. E. et al., 1996, AJ, 112, 1335

Downloaded from http://mnras.oxfordjournals.org/ at Open University Library (PER) on April 13, 2016

© Royal Astronomical Society • Provided by the NASA Astrophysics Data System